

## Hadronic resonances in pp, p–Pb and Pb–Pb in ALICE

Francesca Bellini<sup>1,a</sup> for the ALICE Collaboration

<sup>1</sup>Università degli Studi and INFN - Sez. di Bologna

**Abstract.** The production of hadronic resonances has been measured by the ALICE experiment at mid-rapidity in different collision systems (pp, p–Pb, and Pb–Pb). The measurements of  $K(892)^{*0}$  and  $\phi(1020)$  production in Pb–Pb collisions at  $\sqrt{s_{NN}} = 2.76$  TeV and in pp at  $\sqrt{s} = 2.76$  and 7 TeV are complemented by the more recent measurement in p–Pb collisions at  $\sqrt{s_{NN}} = 5.02$  TeV. The ratios of resonance to long lived hadron production in the three collision systems are compared in order to investigate re-scattering effects, which appear to be relevant for  $K^{*0}$  in the most central Pb–Pb collisions, while  $\phi$  behaves instead like a long-lived particle. Resonance observables contribute to draw the picture of central Pb–Pb collisions as a hydrodynamics-driven system. The comparison of the  $\phi/p$  and  $p/\pi$  ratios as a function of transverse momentum ( $p_T$ ) indicates that the mass of the particle determines the spectral shapes at low and intermediate  $p_T$  in central Pb–Pb collisions. The mean transverse momentum,  $\langle p_T \rangle$ , of  $K^{*0}$  and  $\phi$  in central Pb–Pb collisions is consistent with that of the proton, which has similar mass. In pp and p–Pb collisions the  $\langle p_T \rangle$  of resonances does not follow mass ordering. The nuclear modification factors ( $R_{AA}$ ,  $R_{pA}$ ) of the  $\phi$  meson are also discussed in comparison with those of the stable hadrons.

### 1 Introduction

The ALICE experiment [1] at the LHC has measured  $K(892)^{*0}$  and  $\phi(1020)$  resonance production in pp collisions at  $\sqrt{s} = 2.76$  TeV and 7 TeV [3], in Pb–Pb collisions at  $\sqrt{s_{NN}} = 2.76$  TeV [4], and in p–Pb collisions at  $\sqrt{s_{NN}} = 5.02$  TeV [5] using the data collected during the Run I of the LHC. Note that throughout this paper, the average between  $K(892)^{*0}$  and its antiparticle will be denoted as  $K^{*0}$ , whereas  $\phi(1020)$  will be denoted as  $\phi$ .

In heavy-ion collisions resonances are probes for the different stages of the evolution of the medium. Several observables can be obtained, starting with the measurement of particle spectra, which provide insights into particle production mechanisms. Results in pp and p–Pb collisions constitute the necessary baseline for the measurements in Pb–Pb collisions. In particular, the measurements in pp are the reference for obtaining the nuclear modification factors ( $R_{pPb}$ ,  $R_{AA}$ ), while the p–Pb data help to distinguish genuine effects due to the presence of the hot Quark-Gluon Plasma from those related to the presence of a nuclear target beam, also referred to as cold nuclear matter effects.

Resonances produced in the high energy collisions have very short lifetimes, between a few units and a few tenths of  $fm/c$ , which are comparable with that of the fireball produced in the collision, estimated to be of order of  $10 fm/c$  at the LHC [6]. Considering that lifetime of  $K^{*0}$ ,  $\tau_{K^{*0}}$ , is of the order

---

<sup>a</sup>e-mail: fbellini@cern.ch

of 4 fm/c and  $\phi(1020)$  has a lifetime nearly ten times larger,  $\tau_\phi \sim 45$  fm/c, these particles are excellent probes of the hadronic phase of the collision. Resonances that decay before kinetic freeze-out may not be reconstructed due to the re-scattering of their daughter particles with the hadronic medium, but on the other hand their yield can be regenerated by pseudo-elastic interactions in the fireball. The fraction of “undetected” particles depends on the time span between the chemical and the kinetic freeze-out, the system size, the resonance phase space distribution and the hadronic interaction cross section of the decay products, whereas regeneration is driven by the cross-section of the interacting hadrons. In order to gain insights about these competing effects, ALICE has measured ratios of resonance yield to stable hadrons. Moreover, information on particle formation mechanisms and the dynamical evolution of the system can be inferred by comparing the production of resonances and long lived hadrons with similar mass but different baryon number and strangeness content, in terms of particle yields and mean transverse momentum. Finally, in Pb–Pb, the measurement of resonance production at high transverse momentum ( $p_T$ ), and in particular that of  $\phi$  with its hidden strangeness content, also contributes to the systematic study of in-medium parton energy loss and its flavour dependence.

## 2 Resonance reconstruction in ALICE

ALICE has measured  $K^{*0}$  resonance and  $\phi$  meson production at mid-rapidity by reconstructing their hadronic decay channels,  $K^{*0} \rightarrow K^+ \pi^-$ ,  $\overline{K^{*0}} \rightarrow K^- \pi^+$  and  $\phi \rightarrow K^+ K^-$ . In pp and Pb–Pb collisions the measurements cover one unit of rapidity,  $|y| < 0.5$  in the centre-of-mass reference frame. In p–Pb the rapidity range is restricted to  $-0.5 < y < 0$  in order to ensure the best detector acceptance while the centre-of-mass of the asymmetric collision system moves in the direction of the proton beam.

As summarised in Table 1, the results in pp collisions have been obtained from a sample of  $\sim 3.2 \times 10^7$  minimum bias pp at  $\sqrt{s} = 7$  TeV events from the 2010 dataset, and the full sample of pp collisions at  $\sqrt{s} = 2.76$  TeV from the 2011 dataset, with  $\sim 5 \times 10^7$  minimum bias events. For the analysis of Pb–Pb at  $\sqrt{s_{NN}} = 2.76$  TeV data, a sample of  $\sim 1.3 \times 10^7$  minimum bias events from year 2010 and a sample of  $\sim 4 \times 10^7$  events collected in year 2011, including central, semi-central and minimum bias triggered events, were used. These correspond to the full available datasets. Finally, the dataset of p–Pb collisions at  $\sqrt{s_{NN}} = 5.02$  TeV from year 2013 consists of about  $\sim 9 \times 10^7$  minimum bias events.

**Table 1.** Overview of the data samples analyzed for the measurements of  $K^{*0}$  resonance and  $\phi$  meson production presented in this paper. The total number of events in the minimum bias sample is reported, except for the year 2011 Pb–Pb dataset, where also central and semi-central triggered events are included.

Year	Collision system	Number of events
2010	pp, $\sqrt{s} = 7$ TeV	$3.2 \times 10^7$
2011	pp, $\sqrt{s} = 2.76$ TeV	$5 \times 10^7$
2010	Pb–Pb, $\sqrt{s_{NN}} = 2.76$ TeV	$1.3 \times 10^7$
2011	Pb–Pb, $\sqrt{s_{NN}} = 2.76$ TeV	$4 \times 10^7$
2013	p–Pb, $\sqrt{s_{NN}} = 5.02$ TeV	$9 \times 10^7$

A few technical details relevant for the analyses are presented here, while a reader interested in a full discussion of the performance of the ALICE detector during the Run I of the LHC should refer

to [2]. The trigger and the definitions of centrality and multiplicity classes, respectively in Pb–Pb [7] and p–Pb [8] collisions, are obtained by using the V0 scintillator detectors, covering  $2.8 < \eta < 5.1$  (V0A) and  $-3.7 < \eta < -1.7$  (V0C). The Inner Tracking System (ITS) and Time-Projection Chamber (TPC) provide the reconstruction of the primary vertex of the collision and the global tracking in the ALICE central barrel ( $|\eta| < 0.9$ ). Charged tracks that come from the primary vertex and satisfy good reconstruction quality criteria are selected and identified as pions or kaons via the measurement of the specific ionization energy loss ( $dE/dx$ ) in the TPC. When available (for about 70% of charged particles), information from the Time-Of-Flight (TOF) detector is preferred to that of TPC for the identification of charged K and  $\pi$  in p–Pb, leading to an improvement of the significance of the signal. Resonance signals are extracted starting from the identified decay products by means of an invariant mass analysis: the combinatorial background, estimated by event-mixing or like-sign techniques, is subtracted from the invariant mass spectrum of all primary track pairs of opposite charge. The position and the width of  $K^{*0}(\phi)$  have been extracted by fitting the background-subtracted distribution with a relativistic Breit-Wigner (Voigtian) function for the signal, plus a polynomial to describe the residual background. In all collision systems, the mass and width of  $K^{*0}$  and  $\phi$  are found to be consistent with the values from Monte Carlo simulations and compatible with the vacuum values. In particular, in Pb–Pb collisions no mass shift or broadening has been observed.

### 3 Results and discussion

The published ALICE results on resonance production in pp and Pb–Pb collisions can be found in [3, 4]. Preliminary results on  $K^{*0}(\phi)$  production in p–Pb collisions, including particle yields in the  $p_T$  range  $0 < p_T < 15$  GeV/c ( $0.3 < p_T < 16$  GeV/c) for different V0A multiplicity event classes,

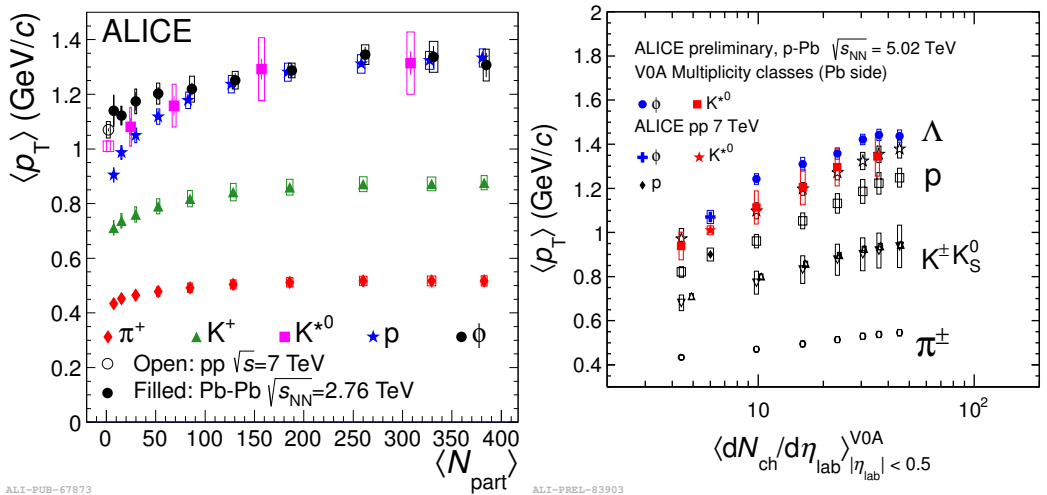


**Figure 1.** Left panel: Mean transverse momentum ( $\langle p_T \rangle$ ) of  $\pi$ ,  $K$ ,  $K^{*0}$ ,  $p$  and  $\phi$  in Pb–Pb collisions at  $\sqrt{s_{\text{NN}}} = 2.76$  TeV [4, 11] as a function of the average number of participants in the collision. For  $K^{*0}$  and  $\phi$ , also the mean transverse momentum measured in pp collisions [3] is reported. Right panel: Preliminary measurement of  $\langle p_T \rangle$  of  $K^{*0}$  and  $\phi$  as a function of the average charged particle multiplicity density measured in the ALICE central barrel in p–Pb at  $\sqrt{s_{\text{NN}}} = 5.02$  TeV, compared to  $\langle p_T \rangle$  of  $\pi$ ,  $K$ ,  $K_S^0$ ,  $p$  and  $\Lambda$  [12] and pp at  $\sqrt{s} = 7$  TeV [3].

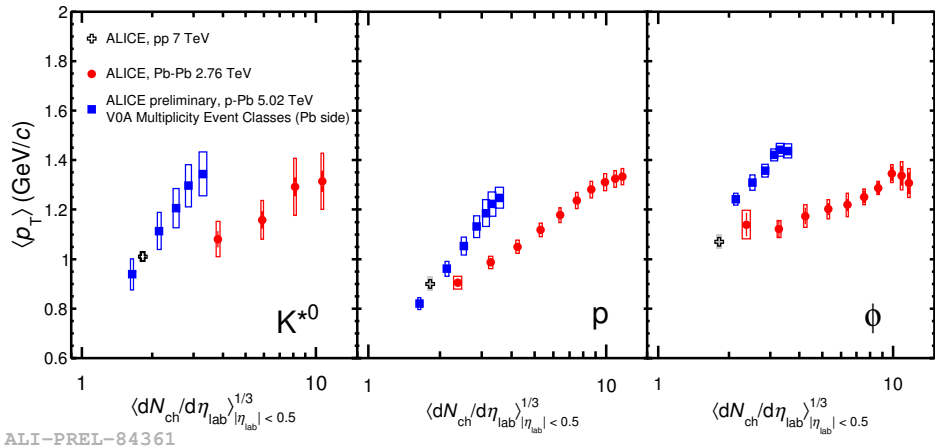


**Figure 2.** System size dependence of the mean transverse momentum of  $K^{*0}$ ,  $p$  and  $\phi$ . The system size is defined as the cube root of the average charged particle multiplicity density measured in the ALICE central barrel in ,  $p$ -Pb at  $\sqrt{s_{\text{NN}}} = 5.02$  TeV (blue) and Pb-Pb at  $\sqrt{s_{\text{NN}}} = 2.76$  TeV (red).

have been reported in [5]. The particle yields are estimated by integrating the corrected spectra in the measured  $p_T$  region. At very low and high  $p_T$ , where no signal can be measured, the yields are extrapolated by integrating a fit function. In p-Pb collisions, the transverse momentum spectra are fitted using a Lévy-Tsallis parameterization [9], whereas a Blast-Wave function [10] is used for Pb-Pb. It may be noted that for  $K^{*0}$  in p-Pb the extrapolated region covers a fraction of the total yield lower than 0.1%, therefore the systematic uncertainty associated with the fit function is negligible, whereas in Pb-Pb the extrapolated yield accounts for the 5.1% of the total. In the same way, the mean  $p_T$  is determined from the measured data points and by using the fitted function only in the extrapolation region.

The mean  $p_T$  of  $K^{*0}$  and  $\phi$  is reported in Figs.1 and 2. The left panel of Fig.1 refers to Pb-Pb collisions and shows the dependence of the  $\langle p_T \rangle$  of resonances and long-lived hadrons on the average number of participant in the collision, thus on centrality. The right panel of Fig.1 reports instead the  $\langle p_T \rangle$  as a function of the average charged multiplicity density in p-Pb and pp collisions. The  $\langle p_T \rangle$  of the resonances and the proton in the three collision systems are directly compared in Fig.2, where they are shown as a function of the cube root of the average charged particle pseudorapidity density, which is considered as a proxy for the system radius [6]. It is observed that particles with similar mass, such as  $K^{*0}$ ,  $p$  and  $\phi$ , have similar  $\langle p_T \rangle$  in the most central Pb-Pb collisions. This observation is consistent with the hypothesis of particle boost in the hadronic phase being driven by radial flow, as also discussed widely in [11]. The “mass-ordering” observed in the most central events for resonances seems to weaken going towards peripheral Pb-Pb collisions and in the smaller collision systems. In p-Pb collisions the  $\langle p_T \rangle$  of resonances increases as a function of the average charged particle multiplicity density, as for other hadrons. However, while  $\langle p_T \rangle$  of long lived hadrons follows mass ordering, the  $\langle p_T \rangle$  of  $K^{*0}$  and  $\phi$  is found to be larger than that of protons.  $\langle p_T \rangle$  of  $\phi$  is also larger than  $\langle p_T \rangle_{\Lambda}$ . This trend is also observed in pp collisions at 7 TeV, where  $\langle p_T \rangle_{\phi} > \langle p_T \rangle_{K^{*0}} > \langle p_T \rangle_p$ . The question remains open whether mesonic resonances deviate from the common trend or the baryons, namely  $p$  and  $\Lambda$ , do instead. The  $\langle p_T \rangle$  in p-Pb shows a steeper increase with multiplicity,  $\langle N_{\text{ch}} \rangle$ , than in Pb-Pb.

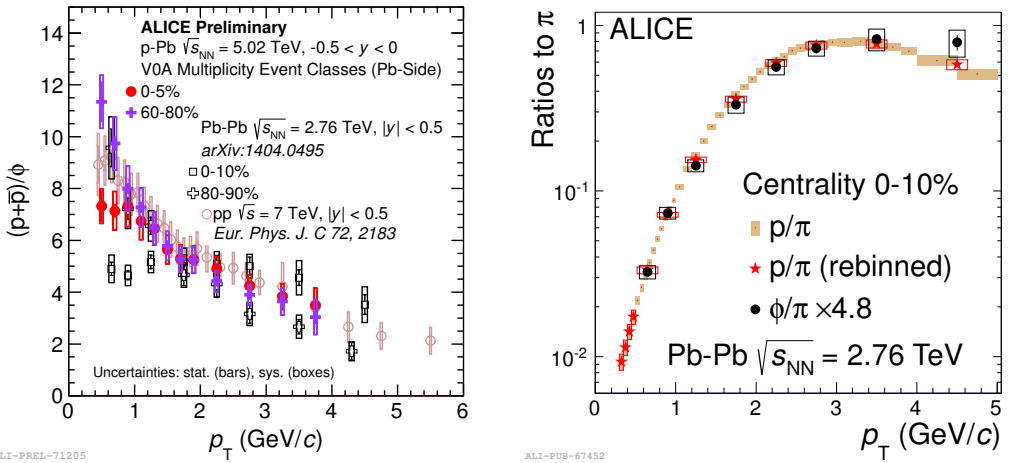


**Figure 3.** Left panel:  $(p+\bar{p})/\phi$  ratio measured in p–Pb in 0–5% and 60–80% V0A multiplicity classes, compared to pp, 0–10% and 80–90% Pb–Pb collisions. Right panel:  $\phi/(\pi^+ + \pi^-)$  compared to the  $(p+\bar{p})/(\pi^+ + \pi^-)$  ratio measured in central (0–10%) Pb–Pb collisions.

This is also observed for unidentified charged particles and discussed in [13], where it is shown that in theoretical models of pp collisions, the strong increase in  $\langle p_T \rangle$  with  $\langle N_{\text{ch}} \rangle$  can be understood as the effect of color reconnection between strings produced in multi-parton interactions [14].

The  $(p+\bar{p})/\phi$  ratio is shown in the left panel of Fig.3 for different centralities. In 0–10% central Pb–Pb collisions this ratio is flat below  $3 \text{ GeV}/c$ . The right panel of Fig.3 reports instead the comparison of the  $\phi/\pi$  and the  $p/\pi$  ratios. The fact that  $p/\pi$  and  $\phi/\pi$  have the same shape as a function of  $p_T$  [4] suggests that the shapes of the  $p_T$  distributions of the  $p$  and  $\phi$  in this momentum range are determined by the particle masses. Incidentally, this is consistent with the observation of mass ordering of  $\langle p_T \rangle$  in central Pb–Pb, attributed to the hydrodynamical behaviour of the system. In peripheral p–Pb and pp collisions the  $p/\phi$  ratio is quantitatively consistent and below  $5 \text{ GeV}/c$  it decreases steeply with  $p_T$ , as in peripheral Pb–Pb collisions. It is noteworthy that the ratio in high-multiplicity p–Pb (0–5% V0A multiplicity event class) is similar to that in 80–90% peripheral Pb–Pb collisions, although for the former a hint of flattening is observed for  $p_T < 1.5 \text{ GeV}/c$ . Fig.4 shows the ratios  $\phi/K$  and  $K^{*0}/K$  measured in p–Pb collisions (in color) compared to the published measurements for pp [3] and Pb–Pb [4]. The  $\phi/K$  ratio is nearly flat across all systems and multiplicities and it reaches the value predicted by a grand-canonical thermal model with  $T = 156 \text{ MeV}$  [15]. On the other hand, the  $K^{*0}/K$  ratio exhibits a decreasing trend towards more central Pb–Pb collisions, where the measured ratio is about 60% of the thermal model value. As more extensively discussed in [4], this can be explained in terms of re-scattering effects, dominating for  $p_T < 2 \text{ GeV}/c$ .

The production of resonances at high transverse momentum in different collision systems is studied through the nuclear modification factors,  $R_{\text{AA}}$  and  $R_{\text{pPb}}$ , defined as

$$R_i(p_T) = \frac{d^2N^i/d\eta dp_T}{\langle T_i \rangle d^2\sigma^{\text{pp}}/d\eta dp_T}, \quad (1)$$

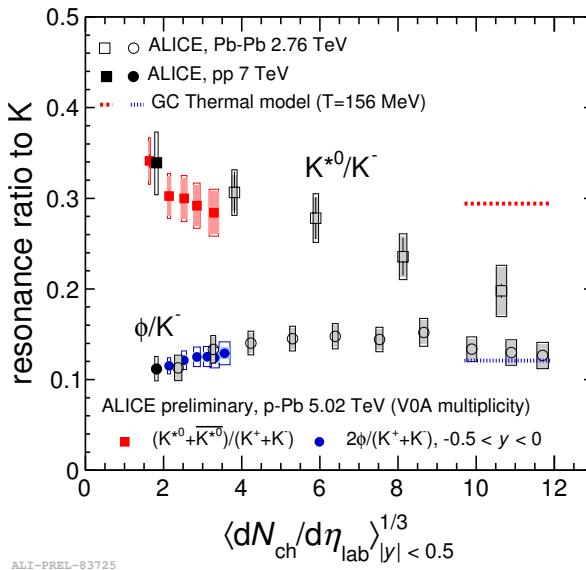


**Figure 4.** Ratio of resonances to charged kaons measured in the three collision systems, as a function of the system size.

namely as the differential yield ( $d^2N^i/d\eta dp_T$ ) in the collision system  $i = \text{AA, p-Pb}$ , relative to the pp reference ( $d^2\sigma^{pp}/d\eta dp_T$ ).  $\langle T_i \rangle$  represents the nuclear overlap function. The existing results on the  $R_{AA}$  of  $\phi$  [16] have been extended up to 21  $\text{GeV}/c$  and measured in finer centrality bins, including in the 0-5% centrality interval, which is reported in the left panel of Fig.5. For the  $R_{AA}$ , the reference spectrum is measured in pp collisions at  $\sqrt{s} = 2.76 \text{ TeV}$ , whereas for  $R_{p\text{Pb}}$ , shown in the right panel of Fig.5, the reference at  $\sqrt{s_{\text{NN}}} = 5.02 \text{ TeV}$  has been obtained by interpolation of the measured cross sections at 2.76 and 7  $\text{TeV}$ , by following the same approach used for charged particles described in [17]. In the momentum region between 2 and 5  $\text{GeV}/c$ , the difference between the  $R_{AA}$  of the  $\phi$  meson and that of the proton is attributed to the different spectral shape of the reference pp spectra, consistently with the observations on the  $p/\phi$  ratio reported in Fig.3. At high- $p_T$  the  $\phi$  meson is strongly suppressed in the most central Pb-Pb collisions with respect to pp collisions. The suppression is consistent with that measured for the stable hadrons, thus supporting once more the observation of the flavour-independence of partonic energy loss in the medium. No suppression is seen at high- $p_T$  in p-Pb collisions compared to pp.

## 4 Conclusions

ALICE results on  $\phi$  and  $K^{*0}$  resonance production at the LHC in all collision systems have been presented at this workshop. The transverse momentum spectra, mean  $p_T$  and particle ratios of resonances to long-lived hadrons have been measured as a function of the multiplicity of the collision and compared in terms of their dependence on the system size. The  $K^{*0}/K$  ratio suggests that in central Pb-Pb collisions,  $K^{*0}$  suffers from re-scattering due to its short lifetime. Instead,  $\phi$  behaves as a long lived particle when compared to the system lifetime. In central Pb-Pb the mean  $p_T$  of resonances is found to be compatible with that of the proton which has similar mass, while in the smaller systems,

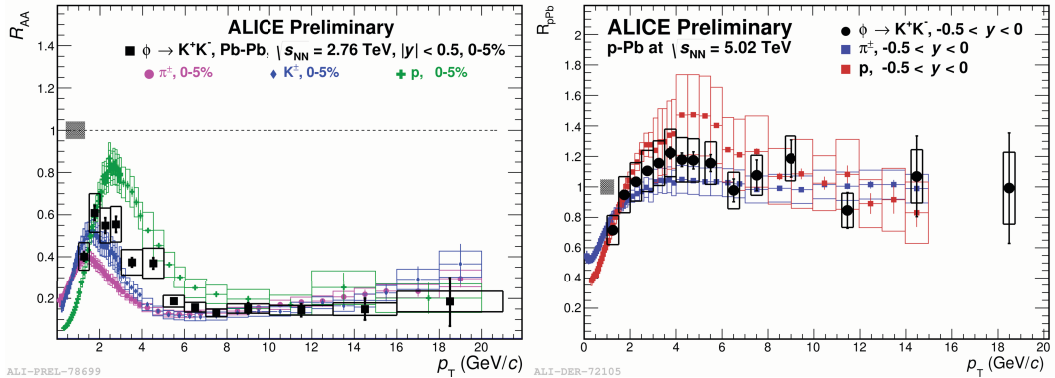


**Figure 5.** Nuclear modification factors of  $\phi$  meson in 0-5% central Pb-Pb collisions ( $R_{AA}$ , left panel) and in minimum bias p-Pb collisions ( $R_{pPb}$ , right panel), compared to that of identified stable hadrons.

pp and p-Pb, it doesn't follow the same mass-ordering as observed in Pb-Pb. The measurement of  $\langle p_T \rangle$  for other hadronic species could shed more light on whether the observed effect is due to the mesonic (baryonic) nature of the particles, or instead, this behaviour is common to resonances rather than long-lived hadrons.

## References

- [1] K. Aamodt *et al.* (ALICE Collaboration), JINST **3**, S08002 (2008)
- [2] B. Abelev *et al.* (ALICE Collaboration), Int. J. Mod. Phys. A **29**, 1430044 (2014)
- [3] B. Abelev *et al.* (ALICE Collaboration), Eur. Phys. J. C **72**, 2183 (2012)
- [4] B. Abelev *et al.* (ALICE Collaboration), arXiv:1404.0495 [hep-ex], *Submitted to Phys. Rev. C*.
- [5] F. Bellini for the ALICE Collaboration, *Proceedings of the Quark Matter 2014 conference*, Nucl. Phys. A **931**, 846–850 (2014)
- [6] K. Aamodt *et al.* (ALICE Collaboration), Phys. Lett. B **696**, 328 (2011)
- [7] B. Abelev *et al.* (ALICE Collaboration), Phys. Rev. Lett. **106**, 032301 (2011)
- [8] A. Toia for the ALICE Collaboration, *Proceedings of the Quark Matter 2014 conference*, Nucl. Phys. A **931**, 315–319 (2014)
- [9] C. Tsallis, J. Stat. Phys. **42**, 479 (1988)
- [10] E. Schnedermann, J. Sollfrank and U. Heinz, Phys. Rev. C **48**, 2462 (1993)
- [11] B. Abelev *et al.* (ALICE Collaboration), Phys. Rev. C **88**, 044910 (2013)
- [12] B. Abelev *et al.* (ALICE Collaboration), Phys. Rev. Lett. B **728**, 25–38 (2014)
- [13] B. Abelev *et al.* (ALICE Collaboration), Phys. Lett. B **727**, 371–380 (2013)
- [14] P.Z. Skands, D. Wicke, Eur. Phys. J. C **52**, 133 (2007)
- [15] J. Stachel, A. Andronic, P. Braun-Munzinger and K. Redlich, J. Phys.: Conf. Ser. **509**, 012019 (2014)
- [16] A. Badalà, EPJ Web of Conferences **66**, 04002 (2014)
- [17] M. Knochel for the ALICE Collaboration, *Proceedings of the Quark Matter 2014 conference*, Nucl. Phys. A **931**, 309–314 (2014)

